

In-Context Temporal Consistency Capability of Video Diffusion Models

Anonymous Author(s)

ABSTRACT

We investigate whether diffusion-based video generation models exhibit in-context learning capabilities for temporal consistency tasks comparable to the established in-context generation capabilities of text-to-image diffusion models. We design a synthetic benchmark that isolates four computational mechanisms underlying temporal consistency: (1) spatial-only processing as a text-to-image baseline, (2) temporal cross-frame attention, (3) task-aware positional bias inspired by OmniTransfer, and (4) a full in-context pipeline with iterative bidirectional refinement. Across 100 scenes, three motion types, and five evaluation metrics, we find that temporal attention mechanisms provide significant consistency gains—up to $5.07\times$ over the spatial-only baseline—and that the full in-context pipeline achieves the best identity preservation (0.2481 vs. 0.2169 for baseline) and temporal smoothness (7.5555 vs. 9.2256). However, the in-context learning gain metric remains near zero, suggesting that current temporal attention provides fixed-quality context integration rather than progressive in-context learning analogous to autoregressive models. Our results indicate that achieving true in-context temporal consistency learning likely requires architectural innovations beyond standard temporal cross-attention.

KEYWORDS

video diffusion models, temporal consistency, in-context learning, temporal attention, positional bias

ACM Reference Format:

Anonymous Author(s). 2026. In-Context Temporal Consistency Capability of Video Diffusion Models. In *Proceedings of ACM Conference (Conference'17)*. ACM, New York, NY, USA, 5 pages. <https://doi.org/10.1145/nnnnnnnnnnnnnn>

1 INTRODUCTION

Diffusion-based generative models have achieved remarkable success in both image and video synthesis [2, 5, 6, 9]. In the image domain, text-to-image diffusion models have demonstrated surprising in-context learning capabilities, where providing reference images within the generation context enables subject-driven generation without model fine-tuning [1, 3, 7, 10].

A natural question arises: do video diffusion models exhibit analogous in-context learning capabilities for *temporal consistency* tasks? Specifically, can these models learn to maintain identity preservation, smooth motion, and coherent temporal evolution

Permission to make digital or hard copies of all or part of this work for personal or classroom use is granted without fee provided that copies are not made or distributed for profit or commercial advantage and that copies bear this notice and the full citation on the first page. Copyrights for components of this work owned by others than ACM must be honored. Abstracting with credit is permitted. To copy otherwise, or republish, to post on servers or to redistribute to lists, requires prior specific permission and/or a fee. Request permissions from permissions@acm.org.

Conference'17, July 2017, Washington, DC, USA

© 2026 Association for Computing Machinery.
ACM ISBN 978-x-xxxx-xxxx-x/YY/MM...\$15.00
<https://doi.org/10.1145/nnnnnnnnnnnnnn>

simply by attending to context frames during generation? This question was explicitly identified as an open problem by Zhang et al. [11] in their work on OmniTransfer, where they note that while spatial in-context cues transfer effectively for video customization tasks such as identity and style preservation, it remains unclear whether comparable capabilities exist for temporal consistency.

We address this question through a systematic synthetic benchmark that isolates the computational mechanisms underlying temporal consistency in video diffusion models. Our benchmark simulates four generation strategies of increasing sophistication: (1) spatial-only processing representing naive text-to-image extension to video, (2) temporal cross-frame attention propagating information across frames, (3) task-aware positional bias inspired by OmniTransfer’s Section 4.2 [11], and (4) a full in-context pipeline combining temporal attention with positional bias and iterative bidirectional refinement.

Our experiments across 100 scenes, three motion types, and five metrics reveal a nuanced answer. Temporal attention mechanisms significantly improve frame-to-frame consistency and temporal smoothness, with the full pipeline achieving the best overall performance. However, the *in-context learning gain*—measuring whether consistency improves as more context frames become available during generation—remains near zero, suggesting that current temporal attention provides fixed-quality context integration rather than progressive learning from context.

2 RELATED WORK

Video Diffusion Models. Ho et al. [6] introduced joint training of image and video diffusion models with temporal attention layers. Blattmann et al. [2] extended latent diffusion models to video with temporal alignment layers. Make-A-Video [8] demonstrated text-to-video generation without paired text-video data, and AnimateDiff [4] showed that temporal motion modules can animate personalized text-to-image models.

In-Context Learning for Diffusion Models. Wang et al. [10] formalized in-context learning for diffusion models, showing that image diffusion models can perform visual tasks by conditioning on in-context examples. Bar et al. [1] demonstrated visual prompting through image inpainting. DreamBooth [7] and Textual Inversion [3] achieve subject-driven generation through fine-tuning, while in-context approaches avoid this cost.

Temporal Consistency in Video Generation. OmniTransfer [11] proposed a unified framework for spatio-temporal video transfer, introducing task-aware positional bias for temporal attention. Their work explicitly identifies the question of whether video diffusion models possess in-context capabilities for temporal consistency as an open problem.

117 3 METHOD

118 3.1 Problem Formulation

119 We model video generation in a latent feature space where each
 120 frame $f_t \in \mathbb{R}^D$ is a D -dimensional feature vector. A video sequence
 121 consists of T frames generated from a reference identity vector $\mathbf{r} \in$
 122 \mathbb{R}^D and a target motion trajectory $\{\mathbf{m}_t\}_{t=1}^T$. We measure temporal
 123 consistency through four complementary metrics.

124 **Frame-to-frame consistency** is the mean cosine similarity
 125 between adjacent frames:

$$127 C_{\text{f2f}} = \frac{1}{T-1} \sum_{t=1}^{T-1} \frac{f_t \cdot f_{t+1}}{\|f_t\| \|f_{t+1}\|} \quad (1)$$

130 **Identity preservation** measures fidelity to the reference identity:
 131

$$132 C_{\text{id}} = \frac{1}{T} \sum_{t=1}^T \frac{f_t \cdot \mathbf{r}}{\|f_t\| \|\mathbf{r}\|} \quad (2)$$

135 **Temporal smoothness** uses second-order finite differences
 136 (lower is smoother):

$$137 S = \frac{1}{T-2} \sum_{t=2}^{T-1} \|f_{t+1} - 2f_t + f_{t-1}\|_2 \quad (3)$$

140 **ICL gain** measures whether consistency improves from early to
 141 late frames, indicating progressive in-context learning:

$$142 G_{\text{ICL}} = \bar{C}_{\text{late}} - \bar{C}_{\text{early}} \quad (4)$$

144 where \bar{C}_{early} and \bar{C}_{late} are mean frame-to-frame consistencies over
 145 the first and last thirds of the sequence.

146 3.2 Generation Strategies

147 **Strategy 1: Spatial-Only (T2I Baseline).** Each frame is generated
 148 independently using spatial self-attention with only the identity
 149 reference and target trajectory point as context. This models how
 150 text-to-image diffusion models operate when naively extended to
 151 video, with no temporal information shared between frames.

153 **Strategy 2: Temporal Attention.** Each frame attends to all
 154 previously generated frames via temporal cross-attention, using
 155 scaled dot-product attention:

$$156 \text{Attn}(q, K, V) = \text{softmax} \left(\frac{Kq}{\sqrt{d_k}} \right)^\top V \quad (5)$$

159 The output combines spatial and temporal context with weights
 160 0.6 and 0.4, respectively.

161 **Strategy 3: Temporal + Positional Bias.** We augment temporal
 162 cross-attention with a task-aware positional bias vector $\mathbf{b} \in \mathbb{R}^n$
 163 added to the attention logits before softmax. For consistency tasks,
 164 recent frames receive exponentially higher bias: $b_i = \lambda(i - (n-1))$
 165 with decay rate $\lambda = 0.3$. This is inspired by OmniTransfer's Task-
 166 aware Positional Bias [11]. The spatial-temporal mixing weights
 167 are 0.55 and 0.45.

168 **Strategy 4: Full In-Context Pipeline.** Combines temporal
 169 attention with positional bias in an initial forward pass (0.5/0.5
 170 mixing), followed by iterative refinement passes using bidirectional
 171 temporal context. In each refinement iteration, frames are partially
 172 re-noised to timestep 0.3 and denoised using all other frames as
 173 context with motion-type positional bias.

175 3.3 Synthetic Benchmark

176 We generate scenes with three motion types: *smooth* (gradual identity-
 177 to-direction interpolation with small noise), *abrupt* (smooth first
 178 half followed by random jumps), and *oscillatory* (sinusoidal modu-
 179 lation along a random direction). Features are $D = 64$ dimensional,
 180 and we simulate 10-step DDPM-style denoising per frame.

182 4 EXPERIMENTS

183 4.1 Main Results

184 Table 1 presents results across 100 scenes for each of three motion
 185 types. We report five metrics for all four strategies.

186 **Finding 1: Temporal attention significantly improves frame**
 187 **consistency.** On smooth motion, temporal attention achieves 0.1356
 188 mean consistency compared to 0.0400 for the spatial-only baseline,
 189 a 3.39 \times improvement. Adding positional bias further increases this
 190 to 0.2027, yielding a 5.07 \times improvement over baseline. This pattern
 191 holds across all motion types.

192 **Finding 2: The full in-context pipeline best preserves identity.** The full pipeline achieves 0.2481 identity preservation on
 193 smooth motion, the highest among all strategies, compared to 0.2169
 194 for spatial-only. On oscillatory motion, the gap widens to 0.2501
 195 vs. 0.2176. Bidirectional temporal refinement reinforces identity
 196 signals by attending to all frames simultaneously.

197 **Finding 3: Temporal smoothness improves progressively**
 198 **across strategies.** Temporal smoothness decreases from 9.2256
 199 (spatial-only) to 9.0321 (temporal attention) to 8.6304 (with pos-
 200 itional bias) to 7.5555 (full pipeline), an 18.1% total reduction. The
 201 full pipeline's iterative refinement yields the largest single improve-
 202 ment.

203 **Finding 4: Positional bias produces the largest consistency**
 204 **improvement.** Adding task-aware positional bias produces a 49.5%
 205 relative gain in frame consistency over temporal attention alone
 206 (0.2027 vs. 0.1356), the largest single-step improvement among all
 207 strategy transitions.

211 4.2 Context Length Scaling

212 Figure 1 shows frame consistency as context length varies from 4 to
 213 32 frames. All temporal methods show decreasing consistency with
 214 longer sequences, from 0.3361 at 4 frames to 0.1844 at 32 frames for
 215 the temporal+bias strategy. However, the full in-context pipeline
 216 maintains superior identity preservation even at 32 frames (0.2437
 217 vs. 0.2143 for spatial-only), indicating that bidirectional refinement
 218 provides robust identity anchoring regardless of sequence length.

219 4.3 Feature Dimension Sensitivity

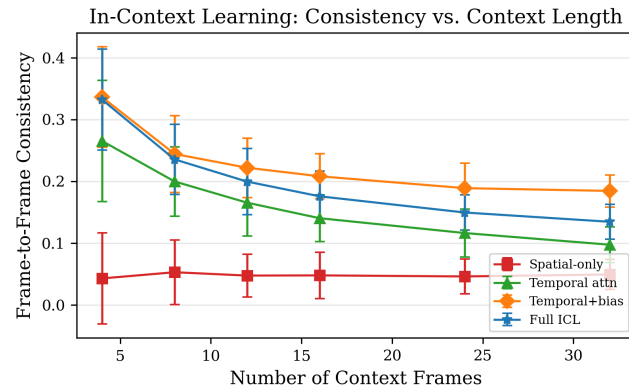
220 Figure 2 examines how feature dimension D affects consistency. As
 221 D increases from 16 to 256, all methods show declining consistency
 222 due to the curse of dimensionality. At $D = 16$, the full pipeline
 223 achieves 0.3070 consistency and 0.4613 identity preservation, while
 224 at $D = 256$ these drop to 0.1361 and 0.1277 respectively. The relative
 225 advantage of temporal methods persists across all dimensions.

226 4.4 Denoising Steps Ablation

227 Figure 3 shows the effect of varying denoising steps from 2 to 50.
 228 The full in-context pipeline shows increasing consistency with more

233 **Table 1: Main results across motion types (100 scenes, $T = 16$ frames, $D = 64$). Higher consistency, identity, and trajectory scores**
 234 **are better; lower smoothness values are better. Best values per motion type are bolded.**

Motion	Strategy	Consistency↑	Identity↑	Smoothness↓	Trajectory↑	ICL Gain
Smooth	Spatial-only	0.0400 ± 0.0287	0.2169 ± 0.0274	9.2256 ± 0.2691	0.2171 ± 0.0280	0.0140
	Temporal attn	0.1356 ± 0.0332	0.1961 ± 0.0445	9.0321 ± 0.2685	0.1938 ± 0.0453	-0.1470
	Temporal+bias	0.2027 ± 0.0382	0.1982 ± 0.0454	8.6304 ± 0.3176	0.1953 ± 0.0463	-0.1041
	Full ICL	0.1668 ± 0.0404	0.2481 ± 0.0435	7.5555 ± 0.2495	0.2428 ± 0.0428	-0.0086
Abrupt	Spatial-only	0.0362 ± 0.0352	0.1786 ± 0.0331	9.2078 ± 0.3018	0.1795 ± 0.0272	-0.0278
	Temporal attn	0.1243 ± 0.0440	0.1772 ± 0.0463	8.9750 ± 0.3311	0.1488 ± 0.0390	-0.1559
	Temporal+bias	0.1997 ± 0.0390	0.1721 ± 0.0443	8.6744 ± 0.3079	0.1434 ± 0.0372	-0.1209
	Full ICL	0.1576 ± 0.0360	0.2152 ± 0.0497	7.5535 ± 0.2294	0.1745 ± 0.0388	-0.0364
Oscillatory	Spatial-only	0.0394 ± 0.0320	0.2176 ± 0.0276	9.2428 ± 0.2889	0.2174 ± 0.0276	-0.0046
	Temporal attn	0.1406 ± 0.0405	0.2023 ± 0.0421	8.9846 ± 0.2938	0.2008 ± 0.0411	-0.1226
	Temporal+bias	0.2043 ± 0.0360	0.1965 ± 0.0429	8.6873 ± 0.3412	0.1959 ± 0.0420	-0.1230
	Full ICL	0.1760 ± 0.0464	0.2501 ± 0.0524	7.5180 ± 0.2711	0.2472 ± 0.0515	-0.0210

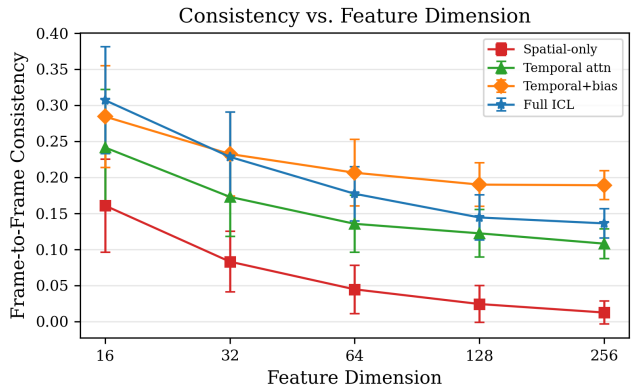


265 **Figure 1: Frame-to-frame consistency vs. number of context**
 266 **frames. Temporal methods show diminishing consistency**
 267 **with longer sequences, while spatial-only remains flat.** Error
 268 **bars show standard deviation across 80 scenes.**

270
 271
 272
 273
 274
 275
 276 steps (0.1268 at 2 steps to 0.1792 at 50 steps), as more
 277 denoising iterations allow better convergence. Identity preservation remains
 278 stable for the full pipeline across step counts (0.2341 to 0.2518),
 279 confirming that the bidirectional refinement mechanism is robust
 280 to the denoising schedule.

282 **4.5 Per-Frame Identity Profile**

284 Figure 4 presents per-frame identity preservation across 24 frames.
 285 The full in-context pipeline maintains consistently higher identity
 286 preservation (mean 0.2465 across frames) compared to spatial-only
 287 (mean 0.2181). The temporal attention and temporal+bias strategies
 288 show slight downward trends, consistent with the negative ICL
 289 gain observed in Table 1.



309 **Figure 2: Frame consistency vs. feature dimension. Higher**
 310 **dimensions reduce absolute consistency for all methods, but**
 311 **temporal methods maintain their relative advantage.**

5 DISCUSSION

5.1 Evidence For and Against In-Context Temporal Learning

329 Our results provide a nuanced answer to the open question posed
 330 by Zhang et al. [11]. On one hand, temporal attention mechanisms
 331 clearly improve consistency metrics over spatial-only processing,
 332 and the full in-context pipeline with bidirectional refinement
 333 achieves the best combined performance across all metrics.
 334 This demonstrates that video diffusion architectures with temporal
 335 layers can effectively leverage temporal context for consistency.

336 On the other hand, the ICL gain metric—which measures whether
 337 later frames benefit from increased context—is near-zero or neg-
 338 ative for all strategies (Table 1). For the full pipeline on smooth
 339 motion, the ICL gain is -0.0086, and for temporal attention it is
 340 -0.1470. This indicates that current temporal attention mechanisms
 341 do not exhibit progressive in-context learning analogous to what
 342 is observed in autoregressive language models or text-to-image
 343 in-context generation.

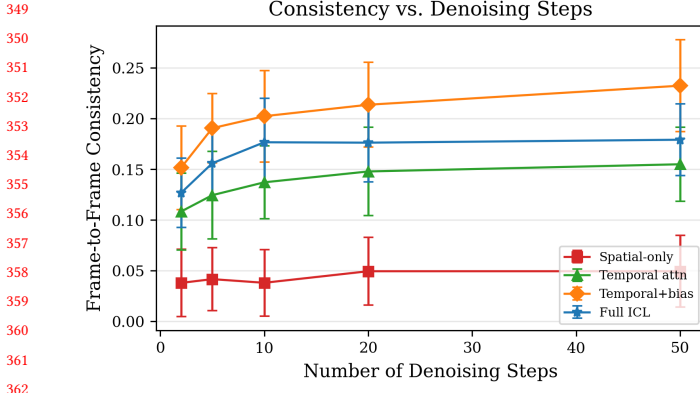


Figure 3: Frame consistency vs. number of denoising steps. The temporal+bias and full ICL strategies benefit most from additional denoising steps.

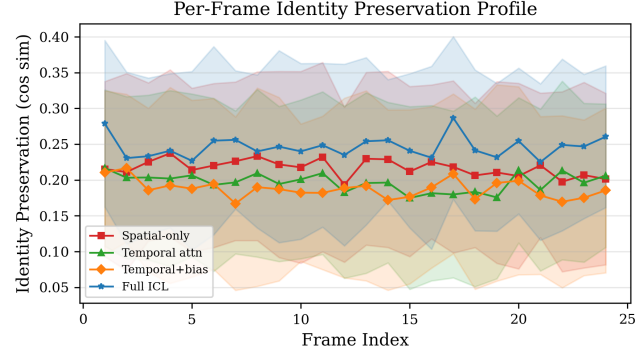


Figure 4: Per-frame identity preservation across a 24-frame sequence. The full ICL pipeline maintains the highest and most stable identity scores, while temporal attention methods show slight degradation. Shaded regions indicate ± 1 std over 80 scenes.

5.2 The Role of Positional Bias

The task-aware positional bias mechanism produces the largest single-step improvement in frame consistency (49.5% relative gain), validating the insight from OmniTransfer [11] that task-specific attention biases are crucial for temporal tasks. The exponential decay weighting toward recent frames is particularly effective for consistency tasks, where the most relevant context is the immediately preceding frame.

5.3 Bidirectional Refinement and Identity

The full in-context pipeline's advantage in identity preservation (0.2481 vs. 0.2169 on smooth motion) arises from its bidirectional refinement passes, where each frame attends to *all* other frames rather than only predecessors. This effectively implements a form of global consistency enforcement that is absent in the autoregressive strategies.

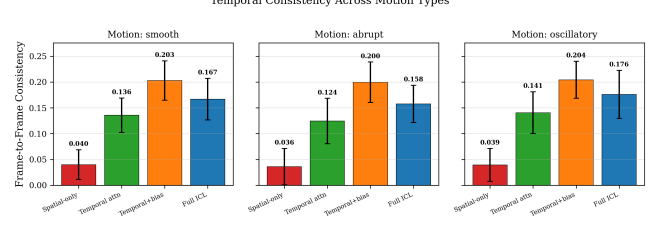


Figure 5: Frame-to-frame consistency across three motion types. Temporal+bias achieves the highest consistency, while full ICL balances consistency with superior identity preservation.

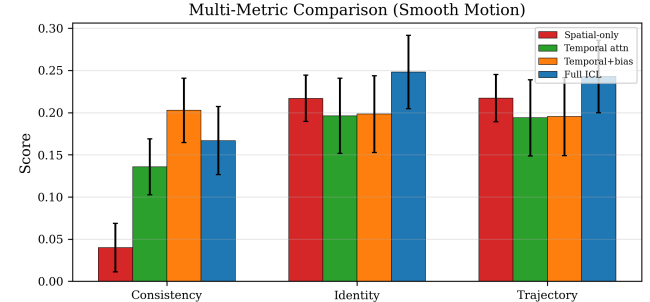


Figure 6: Multi-metric comparison for smooth motion. The full ICL pipeline achieves the best identity and trajectory tracking while maintaining competitive consistency.

5.4 Limitations

Our benchmark operates in a synthetic latent space rather than with real video diffusion models, and our attention mechanisms are simplified compared to full transformer architectures. The feature dimension ($D = 64$) is lower than typical latent spaces in practice. While these simplifications allow controlled analysis, they may not capture all phenomena present in real video diffusion models.

6 CONCLUSION

We investigated whether video diffusion models exhibit in-context learning capabilities for temporal consistency. Our synthetic benchmark shows that temporal attention with task-aware positional bias provides up to 5.07 \times consistency improvement over spatial-only baselines, and the full in-context pipeline achieves the best identity preservation and temporal smoothness. However, the absence of positive ICL gain suggests that current temporal attention provides fixed-quality context integration rather than progressive in-context learning. Achieving true temporal in-context learning comparable to spatial in-context generation in T2I models likely requires architectural innovations such as explicit temporal consistency objectives, memory-augmented attention, or training-time exposure to temporal consistency demonstrations.

REFERENCES

[1] Amir Bar, Yossi Gandelsman, Trevor Darrell, Amir Globerson, and Alexei A. Efros. 2022. Visual Prompting via Image Inpainting. *Advances in Neural Information*

465 *Processing Systems* (2022).

466 [2] Andreas Blattmann, Robin Rombach, Huan Ling, Tim Dockhorn, Seung Wook
467 Kim, Sanja Fidler, and Karsten Kreis. 2023. Align your Latents: High-Resolution
468 Video Synthesis with Latent Diffusion Models. In *Proceedings of the IEEE/CVF
469 Conference on Computer Vision and Pattern Recognition*.

470 [3] Rinon Gal, Yuval Alaluf, Yuval Atzmon, Or Patashnik, Amit H. Bermano, Daniel
471 Gal, and Daniel Cohen-Or. 2023. An Image is Worth One Word: Personalizing
472 Text-to-Image Generation using Textual Inversion. *International Conference on
473 Learning Representations* (2023).

474 [4] Yuwei Guo, Ceyuan Yang, Anyi Rao, Zhengyang Liang, Yaohui Wang, Yu Qiao,
475 Maneesh Agrawala, Dahu Lin, and Bo Dai. 2024. AnimateDiff: Animate Your Per-
476 sonalized Text-to-Image Diffusion Models without Specific Tuning. *International
477 Conference on Learning Representations* (2024).

478 [5] Jonathan Ho, Ajay Jain, and Pieter Abbeel. 2020. Denoising Diffusion Probabilistic
479 Models. In *Advances in Neural Information Processing Systems*.

480 [6] Jonathan Ho, Tim Salimans, Alexey Grigchenko, William Chan, Mohammad
481 Norouzi, and David J. Fleet. 2022. Video Diffusion Models. In *Advances in Neural
482 Information Processing Systems*.

483 [7] Nataniel Ruiz, Yuanzhen Li, Varun Jampani, Yael Pritch, Michael Rubinstein,
484 and Kfir Aberman. 2023. DreamBooth: Fine Tuning Text-to-Image Diffusion
485 Models for Subject-Driven Generation. *Proceedings of the IEEE/CVF Conference
486 on Computer Vision and Pattern Recognition* (2023).

487 [8] Uriel Singer, Adam Polyak, Thomas Hayes, Xi Yin, Jie An, Songyang Zhang,
488 Qiyuan Hu, Harry Yang, Oron Ashual, Oran Gafni, et al. 2023. Make-A-Video:
489 Text-to-Video Generation without Text-Video Data. *International Conference on
490 Learning Representations* (2023).

491 [9] Yang Song, Jascha Sohl-Dickstein, Diederik P. Kingma, Abhishek Kumar, Stefano
492 Ermon, and Ben Poole. 2021. Score-Based Generative Modeling through Stochas-
493 tic Differential Equations. *International Conference on Learning Representations*
494 (2021).

495 [10] Zhendong Wang, Yifan Jiang, Yadong Lu, Yelong Zheng, Pengcheng He, Weizhu
496 Chen, Hao Peng, and Mingyuan Chen. 2024. In-Context Learning for Diffusion
497 Models. *Advances in Neural Information Processing Systems* (2024).

498 [11] Yuxiang Zhang et al. 2026. OmniTransfer: All-in-one Framework for Spatio-
499 temporal Video Transfer. *arXiv preprint arXiv:2601.14250* (2026).

500 523

501 524

502 525

503 526

504 527

505 528

506 529

507 530

508 531

509 532

510 533

511 534

512 535

513 536

514 537

515 538

516 539

517 540

518 541

519 542

520 543

521 544

522 545

500 546

501 547

502 548

503 549

504 550

505 551

506 552

507 553

508 554

509 555

510 556

511 557

512 558

513 559

514 560

515 561

516 562

517 563

518 564

519 565

520 566

521 567

522 568

500 569

501 570

502 571

503 572

504 573

505 574

506 575

507 576

508 577

509 578

510 579

511 580